ACKNOWLEDGMENT

This work was supported under AEC contract AT (40-1)-3913 with David M. Richman as Project Manager.

NOTATION

b = equilibrium change parameter, dimensionless
ΔF = standard free energy of reaction, joules
ΔH = standard heat of reaction, joules
K = equilibrium constant given by Equation (2)
m = dimensionless equilibrium parameter
M = equilibrium constant in Equation (4), mole/g
M' = isotope equilibrium constant analogous to M, ml gas/ml solid
n = number of cycles
R = gas law constant, joules/K
ΔS = standard entropy of reaction, joules/K
t = time, s
T = temperature, K
x = composition of solute in stationary phase, g/g solid
y = composition of solute in mobile phase, g/mole

Greek Letters

ϵ = fractional void volume of column, ml void/ml column
ρ = density, g/ml (for solid) and mole/ml (for gas)

Subscripts

0 = refers to initial column conditions
1, 2 = refer to extreme conditions during cycle
S, F = refer to solid (stationary) and fluid (mobile) phases
n = conditions after n number of cycles

LITERATURE CITED

Jenczewski, T. J., and A. L. Myers, "Separation of Gas Mixtures by Pulsed Adsorption," *Ind. Eng. Chem. Fundamentals*, 9, 216 (1970).

Lappert, M. F., and J. K. Smith, "Thermochemistry of the Complexes of Boron Trifluoride with Dimethyl Sulfoxide and Ethyl Acetate, and the Thermal Decomposition of the Diphenyl Sulfoxide—Boron Trichloride Complex," *J. Chem. Soc.*, 7102 (1965).

Palko, A. A., R. M. Healy, and L. Landau, "Separation of Boron Isotopes II. The BF_3-Anisole System," *J. Phys. Chem.*, 28, 214 (1958).

Palko, A. A., and J. S. Drury, "Fractionation of Boron Isotopes between Boron Trifluoride and Its Molecular Addition Compounds," *J. Chem. Phys.*, 47, 2561 (1967).

———, and W. E. Bull, "Separation of Boron Isotopes V. The Phenol—BF_3 System," *ibid.*, 35, 103 (1961).

Patrick, R. R., J. T. Schrodt, and R. I. Kermode, "Thermal Parametric Pumping of Air-SO_2," *Separation Sci.*, 7, 331 (1972)

Pigford, R. L., B. Baker III, and D. E. Blum, "An Equilibrium Theory of the Parametric Pump," *Ind. Eng. Chem. Fundamentals*, 8, 144 (1969).

Manuscript received March 26, 1975, and accepted March 27, 1975.

Viscoelastic Effect of Polymers on Single Bubble Dynamics

ROBERT Y. TING

Code 6170, Naval Research Laboratory, Washington, D.C. 20375

Single bubble dynamics is involved in many areas of chemical engineering such as evaporative transport of mass or energy, polymer processing technology, and foaming dynamics. Often when the bubbles are formed in environments where polymers are present, polymer viscoelasticity could significantly affect the bubble behavior and in turn the overall flow characteristic. Recently it was reported that high molecular weight polymers added to water could cause suppression of flow-generated cavitation on blunt-nosed bodies (Ellis et al., 1970) as well as jet and propeller cavitations (Hoyt, 1971). The appearance of the cavitation bubble was also changed by the presence of polymer and the bubbles seemed to collapse less violently (Brennen, 1970). While the basic mechanisms involved in these phenomena are not yet known, it was suggested that polymer viscoelasticity may have effects on the growth and collapse of individual cavitation bubbles. Experiments were carried out earlier to observe the growth (Ting and Ellis, 1974) and the collapse (Ellis and Ting, 1974) of individual bubbles in polymer solutions. These experiments indicated that the effect of polymers on single bubble dynamics seemed to be very small. In this report, some theoretical considerations will be given to determine the important parameters through which polymer viscoelasticity may affect the dynamics of single bubbles.

ANALYSIS

Consider the problem of a single bubble growing or collapsing in an incompressible liquid of infinite extent. The vapor bubble is taken to be spherical at all times and gravitational effects are neglected. A thermal equilibrium is assumed such that the vapor pressure inside the bubble is uniform and equal to the equilibrium vapor pressure of the liquid surrounding the bubble at the liquid temperature. Spherical coordinates (r, θ, ϕ) are chosen with the origin at the center of the bubble which is at rest. The only velocity component is in the radial direction, which, in order to satisfy the continuity equation, is generally given as

$$u = \frac{R^2(t)\dot{R}(t)}{r^2} \tag{1}$$

where $R(t)$ is the bubble radius at time t. The equation of motion is

$$\rho\frac{\partial u}{\partial t} + \rho u\frac{\partial u}{\partial r} = -\frac{\partial p}{\partial r} + \frac{\partial \sigma_{rr}}{\partial r} + \frac{2\sigma_{rr} - \sigma_{\theta\theta} - \sigma_{\phi\phi}}{r} \tag{2}$$

where p is the hydrostatic pressure, and σ_{rr}, $\sigma_{\theta\theta}$, and $\sigma_{\phi\phi}$ are the normal stress components. The Oldroyd 3-constant model for a viscoelastic liquid is used (Oldroyd, 1950)

$$\sigma_{ij} + \lambda_1 \left[\frac{\partial \sigma_{ij}}{\partial t} + v_k \frac{\partial \sigma_{ij}}{\partial x_k} + \omega_{ik}\sigma_{kj} + \omega_{jk}\sigma_{ki} - \sigma_{ik}e_{kj} - \sigma_{jk}e_{ki} \right] = 2\eta \left[e_{ij} + \lambda_2 \left(\frac{\partial e_{ij}}{\partial t} + v_k \frac{\partial e_{ij}}{\partial x_k} + \omega_{ik}e_{kj} + \omega_{jk}e_{ki} - 2e_{ik}e_{kj} \right) \right] \quad (3)$$

where σ_{ij}, e_{ij} and ω_{ij} are the stress, strain-rate and vorticity tensor, respectively. This model was chosen because Lumley (1971) has shown that it may be identified with the resulting stress-strain relation derived from the equation of motion of isolated polymer molecules based on the dumbbell model. Of the material constants in Equation (3), η is viscosity, λ_1 a stress relaxation time, and λ_2 a strain relaxation time.

For the present problem, the field is irrotational. So the shear stress components $\sigma_{r\theta}$, $\sigma_{\theta\phi}$, and $\sigma_{r\phi}$ vanish. After a transformation to Lagrangian coordinates (Epstein and Plesset, 1950) $h = [r^3 - R(t)^3]/3$, the normal stress components are determined by using Equations (1) and (3)

$$\frac{d\sigma_{rr}}{dt} + \left(\frac{1}{\lambda_1} + 4\frac{R^2\dot{R}}{r^3} \right) \sigma_{rr} = -\frac{4\eta}{\lambda_1} \cdot \frac{R^2\dot{R}}{r^3} \left[1 + \lambda_2 \left(\frac{\ddot{R}}{\dot{R}} + \frac{2\dot{R}}{R} + \frac{R^2\dot{R}}{r^3} \right) \right] \quad (4)$$

$$\frac{d\sigma_{\phi\phi}}{dt} + \left(\frac{1}{\lambda_1} - 2\frac{R^2\dot{R}}{r^3} \right) \sigma_{\phi\phi} = \frac{2\eta}{\lambda_1} \cdot \frac{R^2\dot{R}}{r^3} \left[1 + \lambda_2 \left(\frac{\ddot{R}}{\dot{R}} + \frac{2\dot{R}}{R} - 5\frac{R^2\dot{R}}{r^3} \right) \right] \quad (5)$$

and $\sigma_{\theta\theta} = \sigma_{\phi\phi}$. Equations (4) and (5) are readily integrated to give

$$\sigma_{rr}(h,t) = -\frac{4\eta}{\lambda_1} \int_0^t e^{\frac{\zeta - t}{\lambda_1}} R^2(\zeta)\dot{R}(\zeta) \left\{ \frac{[3h + R^3(\zeta)]^{1/3}}{[3h + R^3(t)]^{4/3}} \right\} \{1 + \lambda_2 M_{rr}(h,\zeta)\} d\zeta \quad (6)$$

$$\sigma_{\phi\phi}(h,t) = \frac{2\eta}{\lambda_1} \int_0^t e^{\frac{\zeta - t}{\lambda_1}} R^2(\zeta)\dot{R}(\zeta) \left\{ \frac{[3h + R^3(t)]^{2/3}}{[3h + R^3(\zeta)]^{5/3}} \right\} \{1 + \lambda_2 M_{\phi\phi}(h,\zeta)\} d\zeta \quad (7)$$

where

$$M_{rr}(h,\zeta) = \frac{\ddot{R}(\zeta)}{\dot{R}(\zeta)} + \frac{2\dot{R}(\zeta)}{R(\zeta)} + \frac{R^2(\zeta)\dot{R}(\zeta)}{3h + R^3(\zeta)} \quad (8)$$

$$M_{\phi\phi}(h,\zeta) = \frac{\ddot{R}(\zeta)}{\dot{R}(\zeta)} + \frac{2\dot{R}(\zeta)}{R(\zeta)} - 5\frac{R^2(\zeta)\dot{R}(\zeta)}{3h + R^3(\zeta)} \quad (9)$$

Substituting Equations (6) and (7) into Equation (2) written in (h,t), and integrating over the range of h from 0 to ∞, the result is

$$\rho \left(R\ddot{R} + \frac{3}{2}\dot{R}^2 \right) + 4\eta \frac{\dot{R}}{R} = P_v - P_a - \frac{2\sigma}{R} + \frac{2\eta}{\lambda_1}(\lambda_1 - \lambda_2) \int_0^t e^{\frac{\zeta - t}{\lambda_1}} \left[\left(1 + \frac{R^3(\zeta)}{R^3(t)} \right) \frac{\ddot{R}(\zeta)}{R(t)} + 3\frac{R^2(\zeta)}{R^4(t)}\dot{R}(\zeta)^2 \right] d\zeta \quad (10)$$

The first term in the integral of Equation (10) is integrated by parts, and by using the condition $\dot{R}(0) = 0$, Equation (10) reduces to

$$\rho \left(RR + \frac{3}{2}R^2 \right) + 4\eta \frac{\lambda_2}{\lambda_1}\frac{\dot{R}}{R} + P_a - P_v + \frac{2\sigma}{R} = -\frac{2\eta}{\lambda_1}\left(1 - \frac{\lambda_2}{\lambda_1} \right) \int_0^t e^{\frac{\zeta - t}{\lambda_1}} \frac{\dot{R}(\zeta)}{R(t)} \left[1 + \frac{R^3(\zeta)}{R^3(t)} \right] d\zeta \quad (11)$$

The material constants in the Oldroyd model are (Lumley, 1971)

$$\eta = \eta_0(1 + c[\eta]), \quad \lambda_1 = \lambda, \quad \lambda_2 = \lambda/(1 + c[\eta]) \quad (12)$$

where λ is the terminal relaxation time of polymer solutions (Zimm, 1956). Thus, Equation (11) becomes

$$\rho \left(R\ddot{R} + \frac{3}{2}\dot{R}^2 \right) + 4\eta_0 \frac{\dot{R}}{R} + P_a - P_v + \frac{2\sigma}{R} = -\frac{2\eta_0 c[\eta]}{\lambda} \int_0^t e^{\frac{\zeta - t}{\lambda}} \frac{\dot{R}(\zeta)}{R(t)} \left[1 + \frac{R^3(\zeta)}{R^3(t)} \right] d\zeta \quad (13)$$

Now in the case of $c = 0$, the bubble equation for the Newtonian liquid is recovered from Equation (13). The viscous damping term is the same as in the Newtonian case. The viscoelastic memory integral appears to have the opposite sign to the pressure term and hence has an effect of slowing down either the growth or the collapse. It is also noted that the integral is multiplied by a coefficient $\eta_0 c[\eta]/\lambda$. Therefore, for a given species of polymer at certain concentration (that is, c, λ, $[\eta]$ fixed), the viscoelastic effect is scaled with a Reynolds number. Such an effect may be better illustrated by the following analysis:

By introducing the dimensionless variables $\bar{R} = R/R_0$, $\bar{t} = t/t^*$, $\bar{\zeta} = \zeta/t^*$, with $t^* = R_0\sqrt{\rho/\Delta P}$, $\Delta P = |P_a - P_v|$, Equation (13) becomes

$$\bar{R}\bar{R}'' + \frac{3}{2}\bar{R}'^2 + \frac{4}{Re}\frac{\bar{R}'}{\bar{R}} = \pm 1 - \frac{1}{W\bar{R}} - \frac{2}{Re} \cdot \frac{c[\eta]}{D} \int_0^{\bar{t}} e^{\frac{\bar{\zeta} - \bar{t}}{D}} \frac{\bar{R}'(\bar{\zeta})}{\bar{R}(\bar{t})} \left[1 + \frac{\bar{R}^3(\bar{\zeta})}{\bar{R}^3(\bar{t})} \right] d\bar{\zeta} \quad (14)$$

where the positive and the negative signs in the first term on the right-hand side are for the growth and the collapse cases, respectively. Three parameters appear in Equation (14): Reynolds number Re, Weber number W, and Deborah number D. The polymer concentration effect enters the problem as a product $c[\eta]$ in front of the integral. This result will now be briefly discussed.

DISCUSSION

In both the growth and the collapse experiments reported earlier (Ting and Ellis, 1974; Ellis and Ting, 1974), the Reynolds numbers are very high ($Re \approx 0(10^4)$ for the collapse case, and $Re \approx 0(5 \times 10^2)$ for the growth case), and $W >> 1$, $D \approx 0(1)$. Therefore, the magnitude of the viscoelastic correction term as well as that of the viscous damping term is too small compared with the

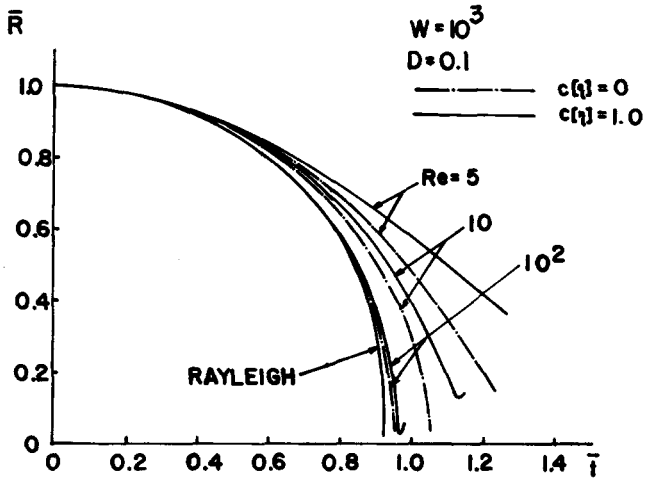

Fig. 1. Effects of Reynolds number and polymer viscoelasticity on bubble collapse.

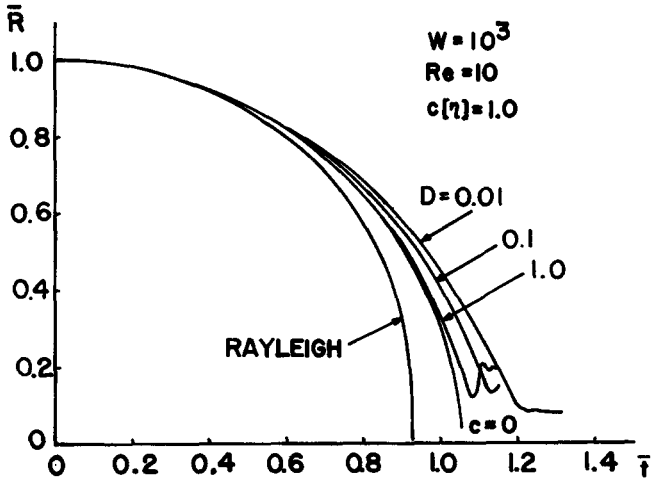

Fig. 2. Effect of Deborah number on bubble collapse.

inertial and pressure terms to be detected by the resolution of the experimental techniques employed.

The effect of polymer viscoelasticity on single bubble dynamics may be demonstrated by numerically solving for $R(t)$ in Equation (14). Since the growth problem involves the cooling effect of the liquid layer surrounding the bubble (Plesset and Zwick, 1958), it requires more detailed analysis and will not be treated here. The retardation effect of polymers on bubble collapse is shown in Figures 1 and 2. In Figure 1 it is seen that bubble collapse is delayed from the Rayleigh inviscid case (Lord Rayleigh, 1971) as Re decreases. The viscoelastic retardation effect is also seen as the non-Newtonian case is compared with the Newtonian viscous case ($c[\eta] = 0$) at the same Reynolds number. The unstable behavior is probably an artifact of the numerical integration technique used and may not reflect the true physical process. The effect of the Deborah number is shown in Figure 2 for the case of $Re = 10$ and $W = 10^3$. As the Deborah number decreases, the collapse time is further increased from the Newtonian case for which the dimensionless collapse time is approximately 1.06. The viscoelastic retardation effect is ordinarily very small during the early stage of the collapse. But the bubble velocity $\bar{R}'$ increases as $\bar{R}$ approaches zero. Therefore, the characteristic strain rate $\bar{R}'/\bar{R}$ in the irrotational field starts from zero and continues to increase as the bubble closes and the magnitude of the viscoelastic correction term in Equation (14) may become appreciable. Consequently, the retardation effect becomes more and more pronounced as the bubble gets smaller and smaller.

There is a growing emphasis on the behaviors of polymers in uniaxial or biaxial elongational flow. In the bubble growth or collapse process each fluid element undergoes biaxial elongation. Especially near the bubble surface, normal stresses will build up to cause the viscoelastic retardation. The material will therefore exhibit an effective viscosity which, sometimes termed *elongational viscosity*, increases with the extensional rate ($\bar{R}'/\bar{R}$) and may become much greater than the Newtonian viscosity (Bird et al., 1970). The analysis here has led to the consideration of a thin film experiment, which hopefully will enable one to demonstrate this high viscous effect. The viscoelastic response of polymeric materials under such biaxial deformations is potentially significant in the fundamental understanding of the flow behavior of polymers.

NOTATION

c = concentration
D = Deborah number, λ/t^*
e_{ij} = strain rate tensor
h = Lagrangian coordinate
P_v = equilibrium vapor pressure
P_a = ambient pressure
p = hydrostatic pressure
r = radial distance from the center of the bubble
R = bubble radius
R_0 = initial bubble radius
$\dot{R}$ = dR/dt
Re = Reynolds number, $\rho R_0^2/\eta_0 t^*$
t = time
t^* = characteristic collapse time, $R_0\sqrt{\rho/\Delta p}$
u = radial velocity component
W = Weber's number, $\rho R_0^3/2\sigma t^{*2}$

Greek Letters

η = solution viscosity
η_0 = solvent viscosity
$[\eta]$ = intrinsic viscosity
θ = polar angle
λ = relaxation time
ρ = liquid density
σ = surface tension
σ_{ij} = stress tensor
ϕ = azimuthal angle
ω_{ij} = vorticity tensor

LITERATURE CITED

Bird, R. B., M. W. Johnson, and J. F. Stevenson, "Molecular Theories of Elongational Viscosity," *Proc. 5th Intern. Congress Rheol.*, 4, 159 (1970).

Brennen, C., "Some Cavitation Experiments with Polymer Solutions," *J. Fluid Mech.*, 44, 51 (1972).

Ellis, A. T., and R. Y. Ting, "Non-Newtonian Effects on Flow Generated Cavitation and on Cavitation in a Pressure Field," *Fluid Mech., Acoustics, and Design of Turbomachinery*, NASA-SP-304, 1, 403 (1974).

Ellis, A. T., J. G. Waugh, and R. Y. Ting, "Cavitation Suppression and Stress Effects in High-Speed Flows of Water with Dilute Macromolecular Additives," *J. Basic Eng.*, 3D, 459 (1970).

Epstein, P. R., and M. S. Plesset, "On the Stability of Gas Bubbles in Liquid-Gas Solutions," *J. Chem. Phys.*, 18, 1505 (1950).

Hoyt, J. W., "Effect of Polymer Additives on Jet Cavitation," *Proc. 16th Am. Towing Tank Conf.*, Sao Paulo, Brazil, **1**, 7 (1971).
Lord Rayleigh, "On the Pressure Developed in a Liquid During the Collapse of a Spherical Cavity," *Philos. Mag.*, **34**, 94 (1917).
Lumley, J. L., "Applicability of the Oldroyd Constitutive Equation to Flow of Dilute Polymer Solutions," *Phys. Fluid*, **14**, 2282 (1971).
Oldroyd, J. G., "On the Formulation of Rheological Equation of State," *Proc. Royal Soc. London*, **A200**, 523 (1950).
Plesset, M. S., and S. A. Zwick, "On the Dynamics of Small Vapor Bubbles in Liquids," *J. Math. Phys.*, **33**, 308 (1958).
Ting, R. Y., and A. T. Ellis, "Bubble Growth in Dilute Polymer Solutions," *Phys. Fluid*, **17**, 1461 (1974).
Zimm, B. H., "Dynamics of Polymer Molecules in Dilute Solutions," *J. Chem. Phys.*, **24**, 269 (1956).

Manuscript received February 10, 1975; revision received and accepted March 31, 1975.

Separation of Isomers via Thermal Parametric Pumping

H. T. CHEN and V. J. D'EMIDIO

Department of Chemical Engineering
New Jersey Institute of Technology, Newark, New Jersey 07102

A recent series of experimental investigations by Chen et al. (1972, 1973, 1974a, 1974b, 1974c) has shown that continuous and semicontinuous parametric pumping can yield very high separation factors in small equipment in a relatively short period of time. In this note we extend our investigation to the separation of isomers. The model system studied is glucose-fructose-water on a cation exchanger (Bio-Rad AG 50W-X4, calcium form). A comparison is made between the experimental data and the calculated results based on the method proposed by Chen et al. (1974a). It should be pointed out that sugar mixtures are notoriously difficult to separate (Hatt and Triffett, 1965) and there has never been a thorough study done on the separation of glucose and fructose even though it might be advantageous industrially in the manufacture of fructose from sucrose via invert sugar.

EXPERIMENT

The experimental apparatus was the same as that used previously (Chen et al., 1972). The feed solution was prepared using reagent grade fructose and glucose obtained from Fisher Scientific Company. Samples for analysis were taken from the product streams at the end of each cycle and analyzed by an automatic polarimeter. For runs involving the binary systems (glucose-water and fructose-water), the analysis was straightforward and the concentration of solute was linearly proportional to the polarimeter reading expressed in angular degree, that is, $R_g^0 = \beta_g \eta_g$ for glucose and $R_f^0 = \beta_f \eta_f$ for fructose (curves 1 and 2 of Figure 1). In the case of the ternary system, glucose-fructose-water, the analysis was somewhat complicated. The R^0 for total sugars (glucose and fructose) was assumed to be the sum of that for glucose and for fructose, that is,

$$R^0 = R_g^0 + R_f^0$$

$$R^0 = \beta_f \eta + \eta_g(\beta_g - \beta_f) \qquad (1)$$

where

$$\eta = \eta_g + \eta_f$$

$$\beta_g = 9.614 \times 10^3$$

$$\beta_f = -16.796 \times 10^3$$

As shown in Equation (1), for a given η_g, a straight line results when R^0 is plotted against η (curve 3 of Figure 1). Thus, knowing η_g one can determine η from R^0 using Equation (1), and the fructose concentration η_f is obtained by subtraction of η_g from η. Note that η_g may be determined by the use of glucostat (Teller, 1956). However, for the present study η_g was found to be constant and equal to the feed concentration (see Results and Discussion).

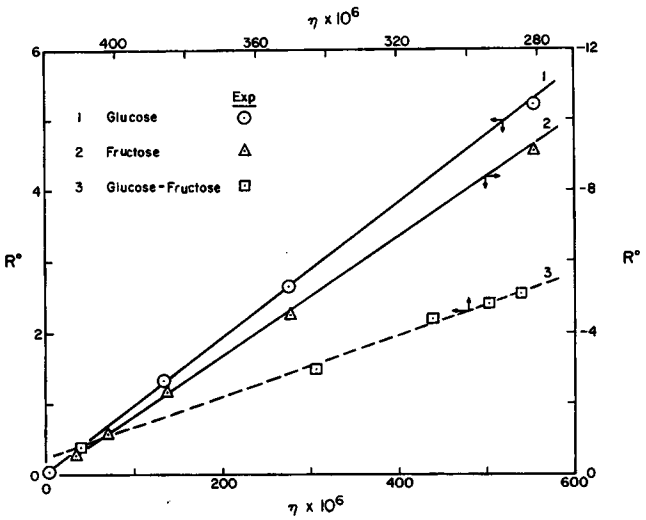

Fig. 1. Relation of angular degree rotation to concentration at ambient temperature (For curve 3, $\eta_g = 277.3 \times 10^{-6}$ g moles/cc).

RESULTS AND DISCUSSION

The experimental parameters are shown in Table 1 and the data are plotted in Figures 2 to 4. The equations previously derived (Chen et al., 1972, 1973) were used to calculate the concentration transients, and computed results corresponding to the experimental runs are also plotted in Figures 2 to 4. These results compare reasonably well with the observed values for both continuous and semicontinuous pump operations. For continuous pump the feed and product streams flow steadily both in upflow and downflow cycles, while the semicontinuous pump is operated batch-wise during upflow and continuously during downflow.

Figure 2 illustrates concentration transients for both glucose and fructose in water. For glucose $\langle y_{TP2} \rangle_n / y_0$